

AD-R193 052

ALKALI IONS WALL RELAXATION IN DICHLORODIMETHYLSILANE  
COATED RESONANCE CEL (U) AEROSPACE CORP EL SEGUNDO CA  
CHEMISTRY AND PHYSICS LAB J C CAMPARO 01 JAN 88

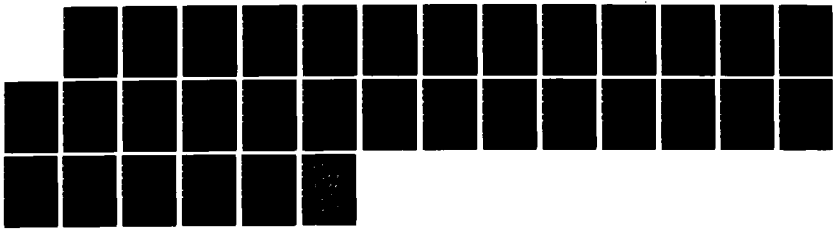
1/1

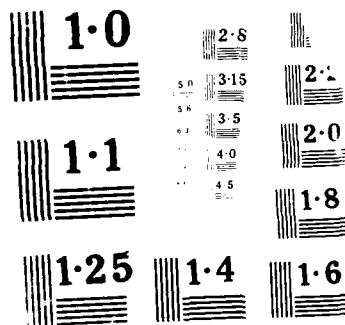
UNCLASSIFIED

TR-0086(6945-05)-4 SD-TR-87-59

F/G 7/3

NL





# Alkali <I•S> Wall Relaxation in Dichlorodimethylsilane Coated Resonance Cells

J. C. CAMPARO  
Chemistry and Physics Laboratory  
Laboratory Operations  
The Aerospace Corporation  
El Segundo, CA 90245

1 January 1988

Prepared for  
SPACE DIVISION  
AIR FORCE SYSTEMS COMMAND  
Los Angeles Air Force Base  
P.O. Box 92960, Worldway Postal Center  
Los Angeles, CA 90009-2960

DTIC  
ELECTRONIC  
PUB. (S)

AD-A193 052

This report was submitted by The Aerospace Corporation, El Segundo, CA 90245, under Contract No. F04701-85-C-0086 with the Space Division, P.O. Box 92960, Worldway Postal Center, Los Angeles, CA 90009-2960. It was reviewed and approved for The Aerospace Corporation by S. Feuerstein, Director, Chemistry and Physics Laboratory.

Lt Michael J. Mitchell CWNZS was the project officer for the Mission-Oriented Investigation and Experimentation (MOIE) Program.

This report has been reviewed by the Public Affairs Office (PAS) and is releasable to the National Technical Information Service (NTIS). At NTIS, it will be available to the general public, including foreign nationals.

This technical report has been reviewed and is approved for publication. Publication of this report does not constitute Air Force approval of the report's findings or conclusions. It is published only for the exchange and stimulation of ideas.

*Michael J. Mitchell*

MICHAEL J. MITCHELL, Lt, USAF  
MOIE Project Officer  
SD/CWNZS

*Joseph Hess*

JOSEPH HESS, GM-15  
Director, AFSTC West Coast Office  
AFSTC/WCO OL-AB

## REPORT DOCUMENTATION PAGE

1a. REPORT SECURITY CLASSIFICATION Unclassified		1b. RESTRICTIVE MARKINGS	
2a. SECURITY CLASSIFICATION AUTHORITY		3. DISTRIBUTION / AVAILABILITY OF REPORT Approved for public release; distribution unlimited.	
2b. DECLASSIFICATION / DOWNGRADING SCHEDULE			
4. PERFORMING ORGANIZATION REPORT NUMBER(S) TR-0086(6945-05)-4		5. MONITORING ORGANIZATION REPORT NUMBER(S) SD-TR-87-59	
6a. NAME OF PERFORMING ORGANIZATION The Aerospace Corporation Laboratory Operations	6b. OFFICE SYMBOL (If applicable)	7a. NAME OF MONITORING ORGANIZATION Space Division	
6c. ADDRESS (City, State, and ZIP Code) El Segundo, CA 90245		7b. ADDRESS (City, State, and ZIP Code) Los Angeles Air Force Base Los Angeles, CA 90009-2960	
8a. NAME OF FUNDING / SPONSORING ORGANIZATION	8b. OFFICE SYMBOL (If applicable)	9. PROCUREMENT INSTRUMENT IDENTIFICATION NUMBER F04701-85-C-0086	
8c. ADDRESS (City, State, and ZIP Code)		10. SOURCE OF FUNDING NUMBERS	
		PROGRAM ELEMENT NO	PROJECT NO
		TASK NO	WORK UNIT ACCESSION NO
11. TITLE (Include Security Classification) Alkali <I-S> Wall Relaxation in Dichlorodimethylsilane Coated Resonance Cells			
12. PERSONAL AUTHOR(S) Camparo, James C.			
13a. TYPE OF REPORT	13b. TIME COVERED FROM _____ TO _____	14. DATE OF REPORT (Year, Month, Day) 1 January 1988	15. PAGE COUNT 27
16. SUPPLEMENTARY NOTATION			
17. COSATI CODES		18. SUBJECT TERMS (Continue on reverse if necessary and identify by block number)	
FIELD	GROUP	SUB-GROUP	
			Atomic Clocks
			Rubidium Frequency Standard
			Polarization Relaxation
			Optical Pumping
19. ABSTRACT (Continue on reverse if necessary and identify by block number)  Alkali <I-S> wall relaxation rates for Pyrex resonance cells coated with dichlorodimethylsilane have been studied. In particular, by considering the ratio of the Rb <sup>85</sup> wall relaxation rate to the Rb <sup>87</sup> wall relaxation rate, evidence is presented showing that dimethylsiloxane surfaces and alkane (paraffin) surfaces relax alkali polarization with similar interaction strengths and correlation times. This conclusion indicates that the outermost functional group of an organic surface molecule has the primary influence on the alkali polarization's surface relaxation.			
20. DISTRIBUTION / AVAILABILITY OF ABSTRACT <input type="checkbox"/> UNCLASSIFIED/UNLIMITED <input checked="" type="checkbox"/> SAME AS RPT <input type="checkbox"/> DTIC USERS		21. ABSTRACT SECURITY CLASSIFICATION Unclassified	
22a. NAME OF RESPONSIBLE INDIVIDUAL		22b. TELEPHONE (Include Area Code)	22c. OFFICE SYMBOL



CONTENTS

PREFACE.....	1
I. INTRODUCTION.....	7
II. THEORY.....	11
III. EXPERIMENT.....	15
IV. RESULTS.....	23
V. DISCUSSION.....	29
VI. SUMMARY.....	33
REFERENCES.....	35

## FIGURES

1.	Schematic Representation of the Reaction Steps for the Chemisorption of Dichlorodimethylsilane to Glass.....	12
2.	Experimental Apparatus.....	16
3.	(a) Schematic Energy Level Diagram for the Two Naturally Occurring Rubidium Isotopes; (b) Absorption Spectrum of Rubidium as Observed in the Coated Resonance Cells.....	17
4.	Sample of the Normalized Probe Intensity Decay and the Resulting Least-Squares Fit to Eq. (5).....	20
5.	Relaxation Rates $\gamma_F^{87}$ as a Function of Normalized Probe Light Intensity.....	24
6.	Relaxation Rates $\gamma_F^{85}$ as a Function of Normalized Probe Light Intensity.....	25

## TABLE

1.	Experimental Results for One Dichlorodimethylsilane Coated Resonance Cell.....	26
----	--	----

## I. INTRODUCTION

Recently, there has been a renewed interest in questions related to the interaction between polarized atomic systems and surfaces.<sup>1,2</sup> This attention stems not only from the intrinsic chemical interest of atom-surface interactions, for example the manner in which various atomic polarization states relax on impact with solid surfaces,<sup>1</sup> but also from a technical interest in developing capabilities to store spin-polarized vapors for H<sup>-</sup> ion sources<sup>3</sup> and atomic frequency standards.<sup>4</sup> As a result of the technical interest, a fair amount of study to date has focused on the interaction between spin-polarized alkali vapors and glass substrates coated with an organic material, specifically, alkanes physisorbed to Pyrex or silane compounds chemisorbed to Pyrex. Quite often these studies take the form of a spin-polarization relaxation experiment, where the rate of relaxation is measured for an alkali atom impacting the coated walls of a Pyrex storage vessel (i.e., a Pyrex resonance cell); and possibly the best example of such a study is the pioneering work of Bouchiat and Brossel.<sup>5</sup>

In the mid-sixties, Bouchiat and Brossel performed a series of elegant experiments investigating the nature of rubidium spin-polarization relaxation on alkane (paraffin) surfaces,<sup>5</sup> and as a result fashioned a clear and simple picture of the general alkali spin-polarization surface relaxation process. According to Bouchiat and Brossel, when an alkali atom impinges on an alkane-like surface and is physisorbed for a time  $\tau_a$ , two uncorrelated interactions work to depolarize the alkali spin. The first interaction was shown to be a magnetic dipole-dipole interaction between the spin of the alkali's valence electron (coupled to the alkali's nuclear spin) and the nuclear spins of the protons on the surface. The second interaction was thought by Bouchiat and Brossel to be of the spin-orbit type, in which the alkali atom would experience a perturbing magnetic field due to the relative motion of the surface carbon atoms. Thus from the alkali atom's perspective its wave function is perturbed during the adsorption by two types of surface related magnetic fields. Furthermore, since surface molecules vibrate, and since a

physisorbed alkali atom may hop from site to site during its adsorption, these magnetic fields will vary randomly in time, implying that each interaction, the dipole-dipole and spin-orbit which will be labeled 1 and 2, respectively, yields a time-dependent perturbation with an associated correlation time  $\tau_{c1}$  and  $\tau_{c2}$ . These correlation times are physically distinct from the adsorption time, since they indicate the time it takes for a specific perturbation to lose information of its past history; the adsorption time on the other hand indicates the total time interval over which the perturbation acts. The correlation times determine the magnitude of each interaction's spectral density at the alkali's resonance frequency. If the correlation times result in a large spectral density at the alkali's resonance, and if the alkali interacts with the perturbing fields for a sufficiently long time, then the surface will be effective in relaxing the alkali's spin-polarization. Thus, it is apparent that surface relaxation rates for alkali spin-polarization depend on the adsorption time of the alkali, the strength of the perturbing magnetic fields, and the perturbing fields' correlation times.

Unfortunately, this picture is incomplete when it comes to interpreting the various surface relaxation phenomena found in the laboratory. For example, drastically different spin-polarization relaxation rates for different samples of the same type of surface have been observed by various authors.<sup>2,6,7</sup> A question therefore arises as to whether these different rates relate to variations in interaction strengths and correlation times, or to differences in the spin-polarized atom's adsorption time. Furthermore, in light of the differences in measured relaxation rates from sample to sample, a second question arises as to the validity of experimental results which indicate the near equivalence of relaxation interactions on various types of alkane-like surfaces.<sup>7</sup> In order to sort out these ambiguities a means of investigating interaction strengths and correlation times independent of the adsorption time is required. In the present series of experiments, investigating the relaxation of rubidium hyperfine polarization (i.e., the observable  $\langle I \cdot S \rangle$ ) on dimethylsiloxane surfaces, the parameter  $\rho$ , defined as the ratio of the  $\text{Rb}^{85}$  surface relaxation rate to the  $\text{Rb}^{87}$  surface relaxation rate, is considered. This parameter will be shown below to depend only on the

various interaction strengths and correlation times, and not on the alkali's surface adsorption time. Measurements of this parameter can therefore be used to resolve some of the remaining ambiguities regarding the surface relaxation of alkali spin-polarization.

One of the purposes of the present study is, therefore, to discern the most likely cause of the disparity among surface relaxation rate measurements for different samples of the same type of surface. Some of the more likely candidates include variations in adsorption time, variations in interaction strengths and/or correlation times, and variations in the degree of substrate coverage by the alkane-like surface. Additionally, it is the purpose of this study to quantify the extent to which different alkane-like surface relaxation interaction strengths and correlation times are equivalent. Since the dimethylsiloxane surface is sufficiently different from the alkane surface studied by Bouchiat and Brossel, yet alkane-like in the sense that the two methyl groups are the outermost functional groups of the surface,<sup>8</sup> a comparison of the  $\rho$  values obtained by Bouchait and Brossel with those obtained in the present study will provide a measure of the equivalence of these quantities between two different types of surface.

## II. THEORY

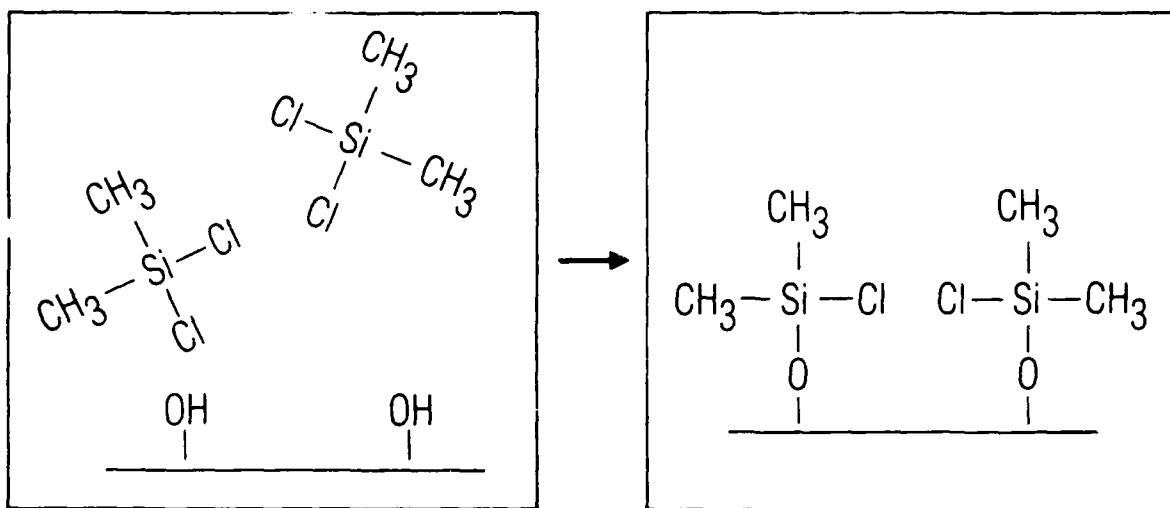
From the work of Bouchiat and Brossel<sup>5</sup> (see also Happer, Ref. 9), the surface relaxation rate of  $\langle I \cdot S \rangle$  on alkane-like surfaces can be written in the form

$$\gamma_S^A = \left(\frac{2\gamma^2}{3}\right) \left(\frac{\tau_a}{\tau_a + \tau_v}\right) \left[ \frac{h_1^2 \tau_{c1}}{1 + (\tau_{c1} W_A)^2} + \frac{h_2^2 \tau_{c2}}{1 + (\tau_{c2} W_A)^2} \right] \quad (1)$$

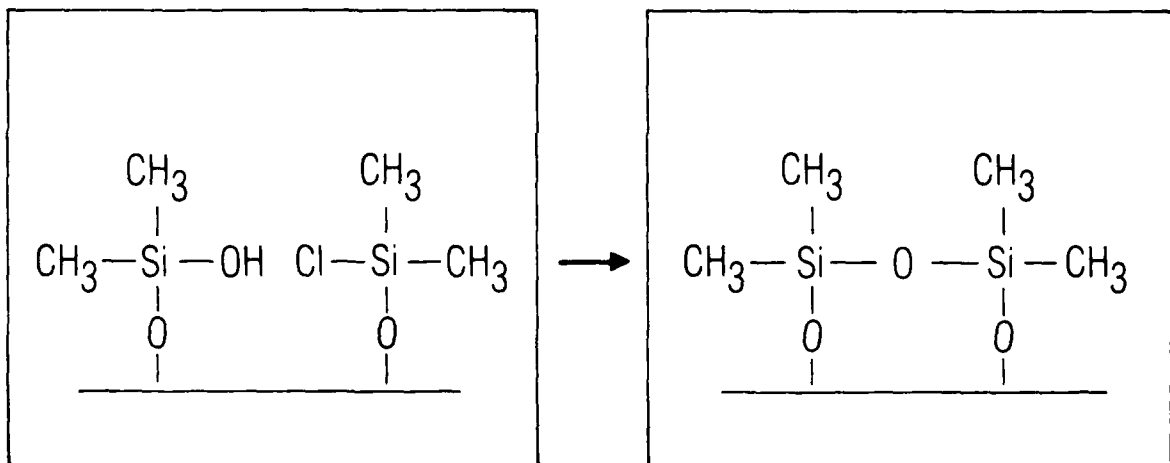
where  $\gamma$  is the gyromagnetic ratio of the electronic angular momentum,  $\tau_v$  is the mean time of flight between alkali-surface collisions, the  $h_i$  and  $\tau_{ci}$  are, respectively, rms magnetic field amplitudes and correlation times of the two interactions, and  $W_A$  is the ground state hyperfine splitting for an alkali isotope of atomic mass  $A$ .  $\tau_a$  is the adsorption time of alkali atoms on the surface, and is the parameter most sensitive to the details of the alkali physisorption (i.e., the adsorption energy).<sup>10</sup> Since for all practical cases of interest  $\tau_a \ll \tau_v$ , and since  $\tau_{c2}$  is of the same order of magnitude as a surface vibrational period (i.e.,  $\tau_{c2} \sim 10^{-12}$  sec  $\ll W_A^{-1}$  for all stable alkali isotopes), Eq. (1) can be simplified to

$$\gamma_S^A = h_1^2 \tau_{c1} \left(\frac{2\gamma^2}{3}\right) \left(\frac{\tau_a}{\tau_v}\right) \left[ \frac{h_2^2 \tau_{c2}}{h_1^2 \tau_{c1}} + \frac{1}{1 + (\tau_{c1} W_A)^2} \right] \quad (2)$$

To a good approximation Eq. (2) should also be valid for alkali spin-polarization relaxation on glass surfaces coated with dichlorodimethylsilane. When dichlorodimethylsilane chemisorbs to glass, a homogeneous siloxane phase is formed on the silica surface by single surface-to-dimethylsilane attachments.<sup>8,11</sup> Essentially, this chemisorption proceeds through multiple steps as illustrated in Fig. 1.<sup>8</sup> In the primary reaction  $\text{Si}(\text{CH}_3)_2\text{Cl}_2$  reacts with silanol hydroxyl groups on the surface, yielding a condensed siloxane phase. In the secondary reaction steps, adsorbed water hydrolyzes some of the unreacted chlorines leading to  $\text{Si}(\text{CH}_3)_2(\text{Cl})(\text{O}-)$  and  $\text{Si}(\text{CH}_3)_2(\text{OH})(\text{O}-)$  species in close proximity. With a slight bond angle adjustment these species can



(a)



(b)

Fig. 1. Schematic Representation of the Reaction Steps for the Chemisorption of Dichlorodimethylsilane to Glass. (1a)  $\text{Si}(\text{CH}_3)_2\text{Cl}_2$  reacts with  $\text{OH}$  groups on the surface yielding  $\text{HCl}$  and a condensed siloxane molecule  $\text{Si}(\text{CH}_3)_2(\text{Cl})(\text{O}-)$ . Subsequent reaction of this siloxane molecule with adsorbed water leads to situations as depicted in 1b. (1b) Adsorbed water has hydrolyzed some of the unreacted chlorines, leading to  $\text{Si}(\text{CH}_3)_2(\text{Cl})(\text{O}-)$  and  $\text{Si}(\text{CH}_3)_2(\text{OH})(\text{O}-)$  species in close proximity. With a slight bond angle adjustment, these neighboring species can react to form  $\text{HCl}$  and the vertically polymerized dimer  $[\text{Si}(\text{CH}_3)_2(\text{O}-)]_2$ .

then react to form the vertically polymerized structure of Fig. 1b. Thus, when an alkali atom impinges on the dimethylsiloxane (DMS) surface it initially interacts with the outermost methyl groups, so that one would expect the surface's polarization relaxation mechanisms to be due to magnetic dipole type interactions and the form of Eq. (2) to hold. However, since both oxygen and silicon are higher  $Z$  elements than carbon, and since spin-orbit relaxation in the gas phase increases as  $Z^3$ ,<sup>12</sup> one might expect an increase in the  $h_2$  parameter for the DMS surface if the alkali atom can get close enough to either of these higher  $Z$  elements.

Considering Eq. (2) it is clear that the relaxation rate is directly proportional to the adsorption time  $\tau_a$ , and a term (in brackets) which contains the information on the polarization relaxation interactions. However, since  $\tau_a$  can depend on the details of the surface coating's preparation,<sup>13</sup> comparisons of raw relaxation rate measurements will always contain a degree of ambiguity. Thus, in order to make a comparison with the results of Bouchiat and Brossel we consider the parameter  $\rho$ , which is the ratio of  $Rb^{85}$  to  $Rb^{87}$  (I.S.) surface relaxation rates

$$\rho \equiv \gamma_s^{85} / \gamma_s^{87} = \frac{B + [1 + (\tau_{c1} w_{85})^2]^{-1}}{B + [1 + (\tau_{c1} w_{87})^2]^{-1}} \quad (3)$$

where  $B = h_2^2 \tau_{c2}^2 / h_1^2 \tau_{c1}^2$ . The advantage of considering this parameter is that it is independent of  $\tau_a$ , yet sensitive to variations in the parameters that describe the (I.S.) relaxation interactions.

### III. EXPERIMENT

In order to measure rubidium isotope  $|I-S\rangle$  wall relaxation rates, an experimental apparatus was constructed, and is shown schematically in Fig. 2. A single-mode Hitachi diode laser, HL 7801E, with a few milliwatts output power and a linewidth of 46 MHz, was tuned to the  $D_2$  resonance of rubidium at 780.2 nm ( $5^2P_{3/2} - 5^2S_{1/2}$ ), and was split into a collimated pump and probe beam. As shown in Fig. 3, the ground state hyperfine splitting of each isotope was clearly resolved by the diode laser. The pump beam was focused onto the blade of a mechanical chopper, and then recollimated before passing through the coated spherical resonance cell. The probe beam was angled slightly with respect to the pump beam, and was attenuated by neutral density filters so that the measured relaxation rates could be extrapolated to zero probe light intensity. The spatial resolution of the pump and probe beams was necessary, because it was found that the pump beam saturated the photodiode and perturbed the relaxation rate measurements.

The mechanical chopper alternately unblocked and blocked the pump beam for equal 5 msec time periods. Since the optical pumping time was  $\sim 0.2$  msec, a steady-state hyperfine polarization was rapidly achieved during the pump-unblocked portion of the chopper's motion. During the pump-blocked portion of the chopper's motion this steady-state hyperfine polarization relaxed towards some small new value determined by the probe light intensity. The relaxation was observed as a transient decrease in the probe beam's transmitted intensity, and was recorded on an LAS 12/70 Nicolet signal averager. The apparent time required for the pump beam to change its state from unblocked to blocked was  $\sim 80$   $\mu$ sec, and this was limited by the electronics associated with signal amplification at the photodiode. Without this amplification the pump beam "turn-off" time could be reduced to 10  $\mu$ sec, which was limited by the speed of the mechanical chopper.

The spherical resonance cell was located inside a solenoid which produced a magnetic field of 2.6 G, oriented parallel to the pump beam propagation direction. Since the laser was linearly polarized to better than 99%, a small

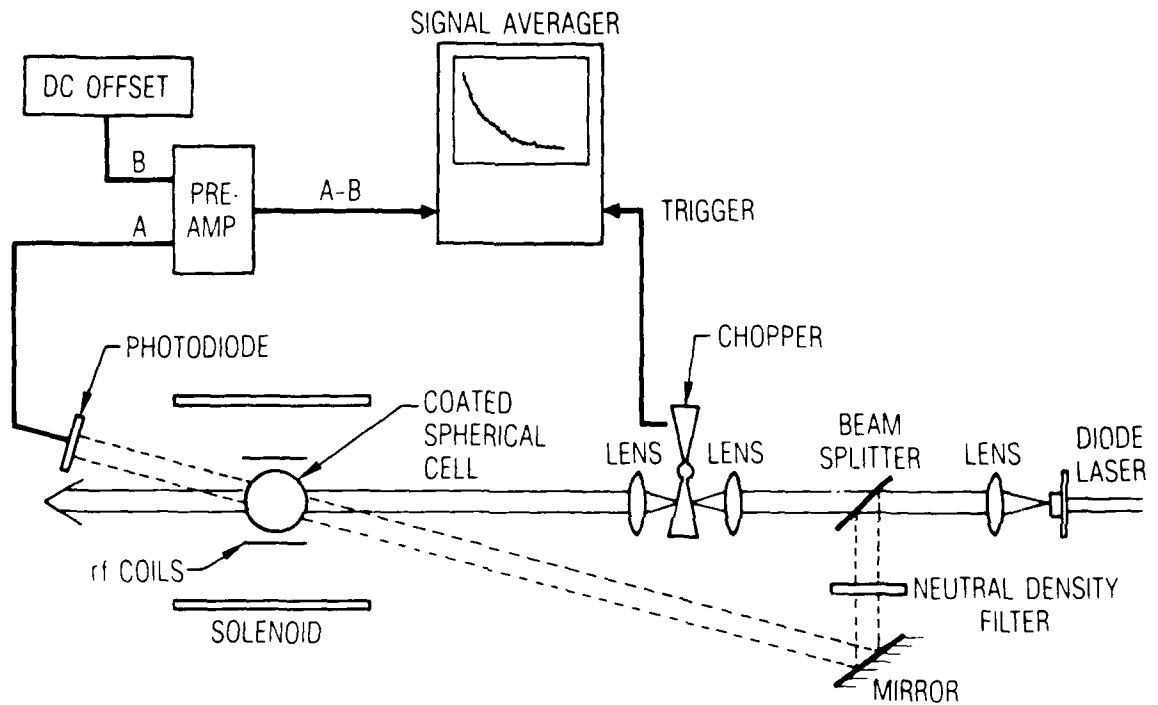


Fig. 2. Experimental Apparatus. The collimated emission from a diode laser was split into a strong pump and weak probe beam. The pump beam produces a hyperfine polarization  $\langle I \cdot S \rangle$  in a rubidium vapor contained in a dichlorodimethylsilane coated resonance cell. When the pump beam is blocked by the motion of the mechanical chopper, the probe beam's transmitted intensity decreases and is indicative of the relaxation of  $\langle I \cdot S \rangle$ .

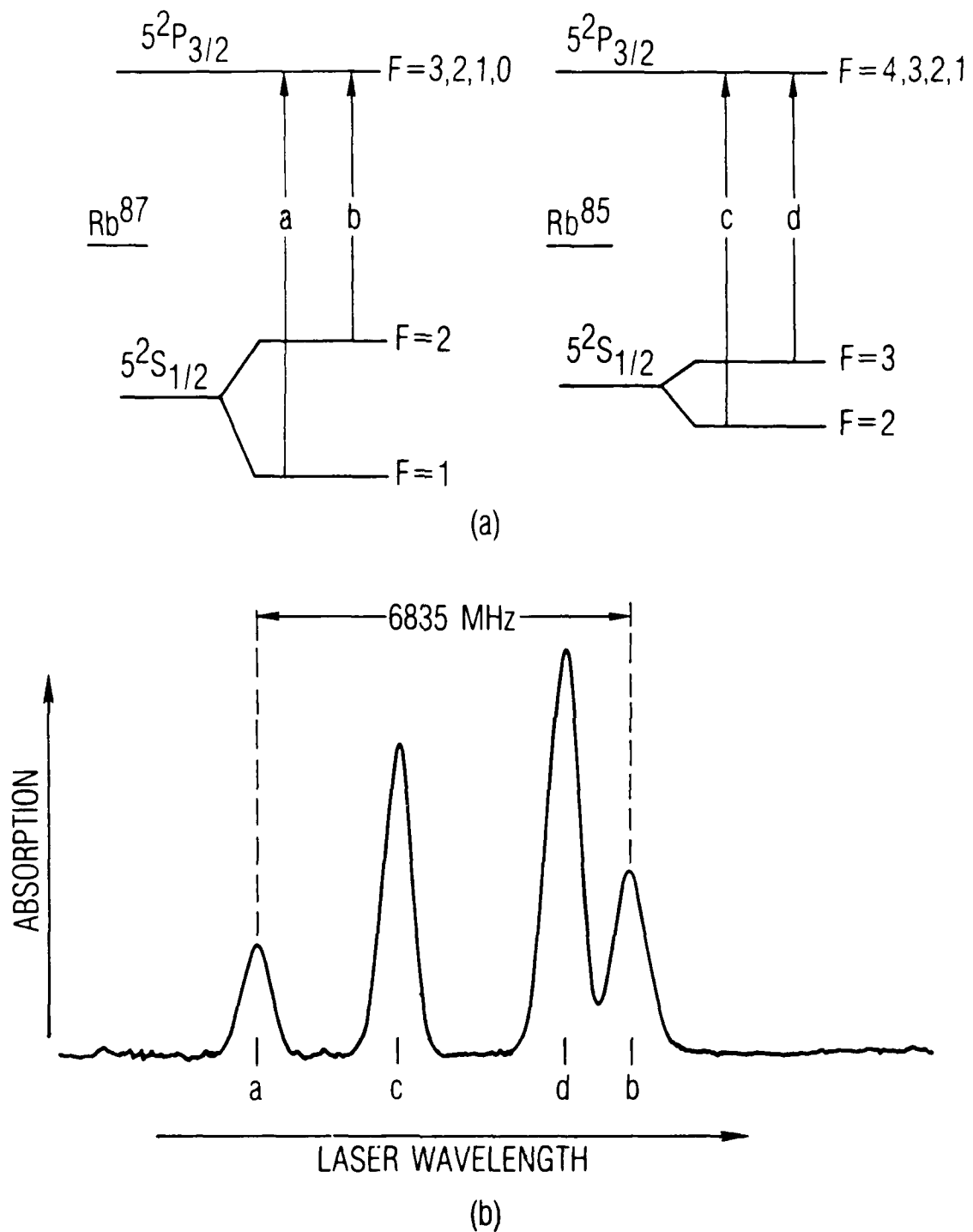


Fig. 3. (a) Schematic Energy Level Diagram for the Two Naturally Occurring Rubidium Isotopes; (b) Absorption Spectrum of Rubidium as Observed in the Coated Resonance Cells. The atomic resonances are labeled in accordance with (a).

atomic spin alignment<sup>14</sup> was created in the vapor by depopulation pumping in addition to the hyperfine polarization  $\langle I \cdot S \rangle$ . By performing magnetic resonance with the rf coils located near the resonance cell, one could observe the effect of this spin alignment on the pump beam transmitted intensity: when the rf field's frequency matched the ground state Larmor frequency of the isotope under study, a small resonant increase in the pump beam's transmitted intensity occurred. The increase in transmitted intensity resulted from the rf-induced population redistribution among the optically excited ground state Zeeman sublevels, which allowed for a greater transfer of population into the nonabsorbing hyperfine multiplet. However, as pointed out by Bouchiat and Brossel,<sup>5</sup> one needs to exercise care in measuring  $\langle I \cdot S \rangle$  relaxation rates when an atomic spin orientation or alignment is present, because the spin alignment relaxation will contribute to the observed probe intensity decay. Since spin alignment and  $\langle I \cdot S \rangle$  do not necessarily relax at the same rate, systematic errors in the determination of  $\langle I \cdot S \rangle$  relaxation rates can result. We therefore studied the influence of a saturating rf field on the measured relaxation rates, and found that the spin alignment contribution to these rates was negligible.

The resonance cells used in the present study were spherical, 1 in. diameter Pyrex cells that had a 1 in. long, 0.3 cm i.d. Pyrex stem attached to one end. The cells were coated with dichlorodimethylsilane using a procedure similar to that of Zeng et al.:<sup>2,15</sup> briefly, a 10% by volume solution of dichlorodimethylsilane in cyclohexane was prepared, inserted into the resonance cells, and shaken; the excess was removed; the cells were rinsed twice with pure cyclohexane, and allowed to dry in air overnight. The cells were then baked out at  $10^{-6}$  Torr and  $130^\circ\text{C}$  for approximately  $2 \frac{1}{2}$  days. After the bakeout, natural rubidium (72%  $\text{Rb}^{85}$  and 28%  $\text{Rb}^{87}$ ) was distilled into the cells.

For the experiment the resonance cells were located vertically inside a wire-wound oven which maintained a vertical temperature gradient of roughly  $6^\circ$ . A visible ring of condensed rubidium could be seen near the tip of the resonance cell's stem, and we estimated that the vapor pressure of rubidium in the spherical portion of the cell was approximately equal to the saturated

vapor pressure existing above a pool of rubidium metal at 29°C. (This is probably an overestimate of the Rb vapor pressure as discussed in Ref. 15.) Using Killian's formula for the saturated vapor pressure of rubidium,<sup>16</sup> this implied a rubidium number density of  $1.8 \times 10^{10} \text{ cm}^{-3}$ .

Defining  $n(t)$  as the time dependent fractional population in the optically absorbing hyperfine multiplet, it is quite easy to show that the transmitted intensity of the probe beam has the form

$$I(t) = I \exp [-n(t)l/d] \quad (4)$$

where  $l$  is the cell length and  $d$  is the optical depth. Since  $\langle I \cdot S \rangle$  is proportional to  $n(t)$ , it follows that  $n(t)$  and  $\langle I \cdot S \rangle$  relax in the same way. From Eq. (4) and the fact that  $n(t)$  increases exponentially with time during the pump blocked time interval,<sup>5</sup> one can show that

$$\ln [I(\tau)/I(t)] = \kappa(1 - \exp[-(t - \tau)\gamma_F^A]) \quad (5)$$

where  $I(\tau)$  is some initial transmitted probe intensity after the pump beam has been blocked ( $t > \tau$ ),  $\kappa$  is a constant, and  $\gamma_F^A$  is the total  $\langle I \cdot S \rangle$  decay rate probing the  $F = a = I + 1/2$  or  $F = b = I - 1/2$  hyperfine multiplet. For each transmitted intensity transient, 20 data points were digitized and fit by a least squares procedure to Eq. (5) in order to determine  $\gamma_F^A$ . A sample of the data and the resulting fit is shown in Fig. 4.

For completeness the laser was tuned to each of the four isotopic resonances, and the relaxation rate  $\gamma_F^A$  was measured as a function of normalized probe light intensity ( $I/I_0$ )

$$\gamma_F^A = k_F^A (I/I_0) + \gamma_0^A \quad (6)$$

In this expression  $k_F^A$  is the rate of change of the measured relaxation rate with normalized probe light intensity, and  $\gamma_0^A$  is the light-independent relaxation rate. The slope  $k_F^A$  depends on the probed hyperfine level, because the rate of depopulation pumping depends on the total ground state degeneracy and

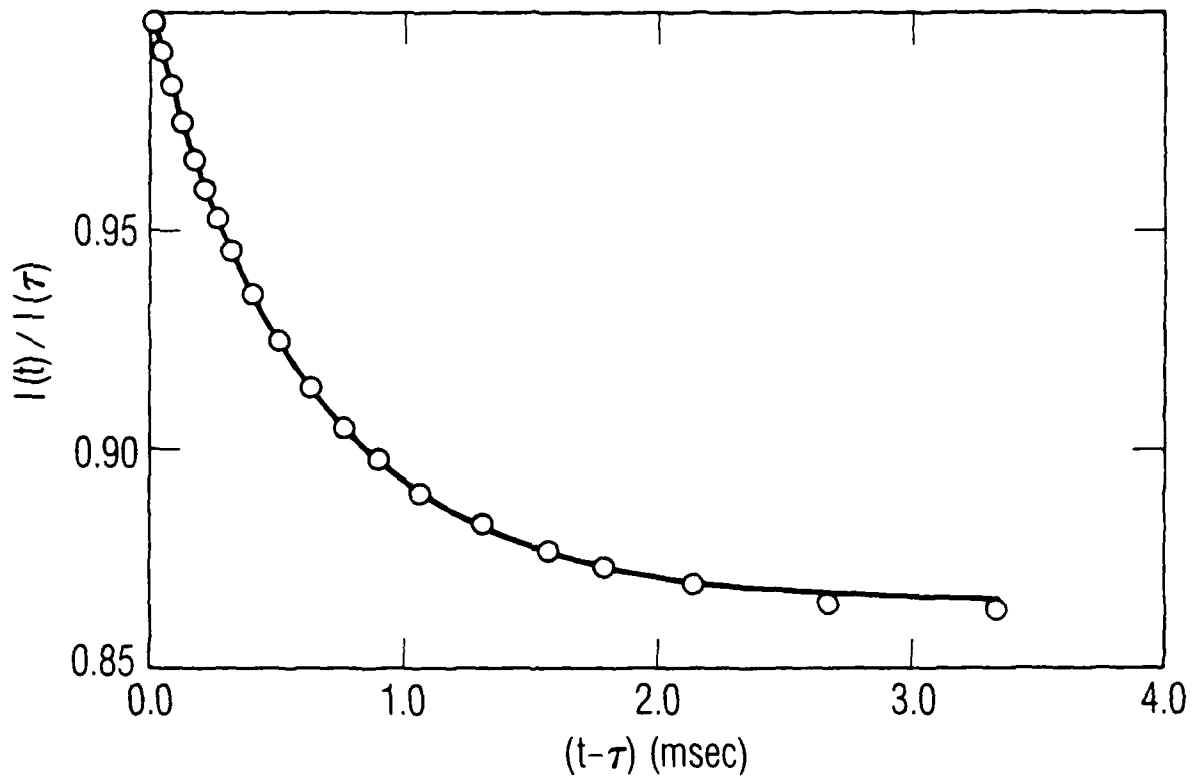


Fig. 4. Sample of the Normalized Probe Intensity Decay and the Resulting Least-Squares Fit (Solid Line) to Eq. (5)

the degeneracy of the optically absorbing hyperfine level. Theoretically, it can be shown that the ratio of the two slopes is a simple function of the alkali nuclear spin:  $k_a^A/k_b^A = 1/(I + 1)$ .<sup>17</sup> However, one can show quite generally by microscopic reversibility arguments that  $\gamma_0^A$  must be independent of the probed hyperfine level. Thus, the ratio of the slopes and the equality of  $\gamma_0^A$  values obtained by probing the two ground state hyperfine levels of a particular isotope acted as a check on the experimental results and their analysis.

#### IV. RESULTS

Figures 5 and 6 show the measured relaxation rates  $\gamma_F^A$  for one coated resonance cell as a function of relative probe intensity for  $\text{Rb}^{87}$  and  $\text{Rb}^{85}$ , respectively. The solid line is a linear least-squares fit of the data yielding the slope  $k_F^A$  and the intercept  $\gamma_O^A$ . It is clear from the figures that, as anticipated, the slopes depend on the probed hyperfine level  $F$ , and that the relaxation rates extrapolate to the same value. Furthermore, the ratios of the slopes as determined by the least-squares fit are in very good agreement with the theoretical expression. Values of the quantities  $k_F^A$  and  $\gamma_O^A$  for this cell are collected in Table 1.

The light-independent relaxation rates collected in the table, however, are not due solely to wall relaxation. Actually, they contain contributions arising from two additional mechanisms

$$\gamma_O^A = \gamma_{\text{ex}} + \gamma_{\text{st}} + \gamma_S^A \quad (7)$$

where  $\gamma_{\text{ex}}$  is the spin exchange relaxation rate of  $\langle I \cdot S \rangle$ , and  $\gamma_{\text{st}}$  is the rate at which atoms collide with the stem region and impact the ring of condensed rubidium (immediately depolarizing on impact). Since spin exchange and stem relaxation will show no isotope specificity, any isotopic difference in  $\langle I \cdot S \rangle$  relaxation rates should be attributed to the surface relaxation mechanism alone.

From our estimate of the alkali density and knowledge of the spin exchange cross section<sup>18</sup> we find that  $\gamma_{\text{ex}} \sim 10 \text{ sec}^{-1}$ . In order to estimate  $\gamma_{\text{st}}$  we assume that the probability of colliding with the stem region is equal to the fractional surface area covered by the stem region:  $\gamma_{\text{st}} = \bar{v}r^2/4R^3$ , where  $\bar{v}$  is the average thermal velocity of a rubidium atom,  $r$  is the cross sectional radius of the stem region, and  $R$  is the radius of the spherical cell; in this way we estimate  $\gamma_{\text{st}}$  as  $78 \text{ sec}^{-1}$ . Thus, as rough as these estimates are, it is clear that the surface relaxation is the dominant contribution to  $\gamma_O^A$ , and for the cell of Figs. 5 and 6 one obtains  $\gamma_S^{85} = 760$

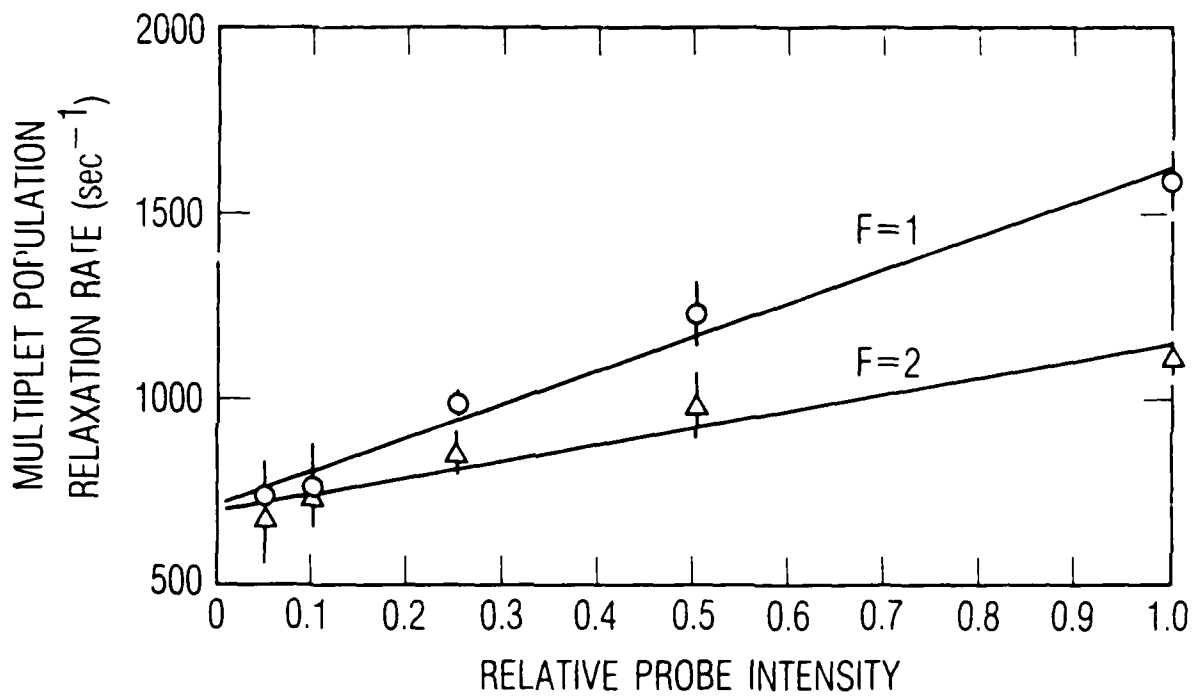


Fig. 5. Relaxation Rates  $\gamma_F^{87}$  as a Function of Normalized Probe Light Intensity. The solid lines are least-squares fits to the data for the cases of probing the population in either the  $F = 1$  or  $F = 2$  hyperfine level.

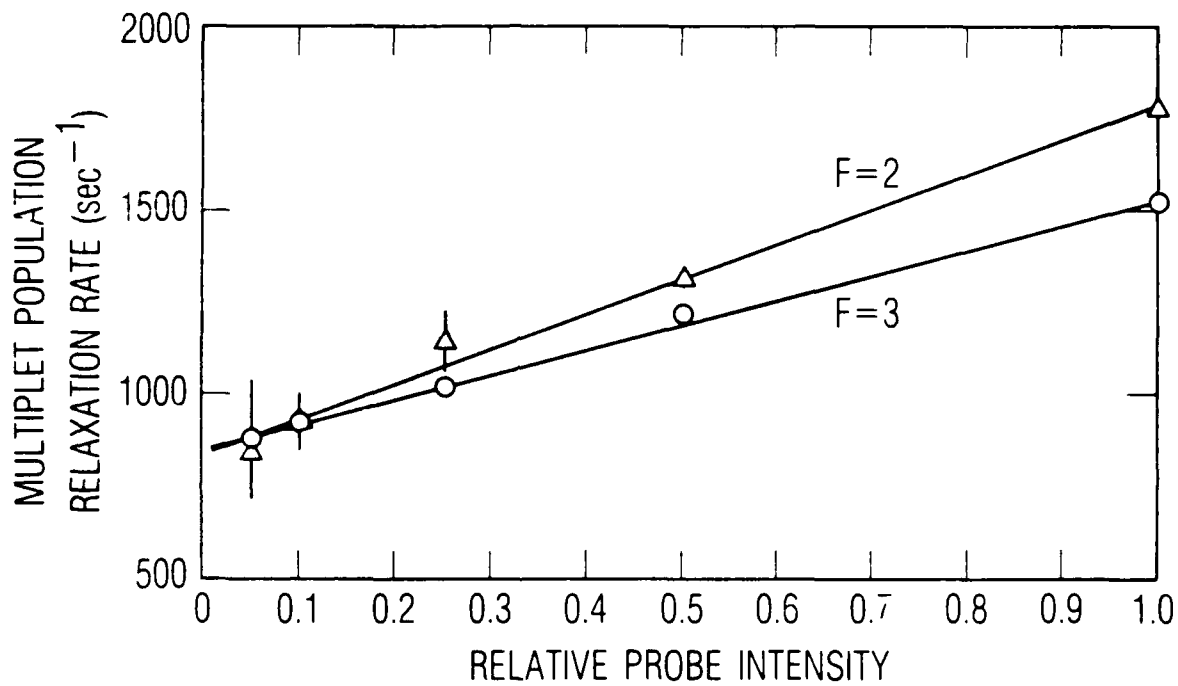


Fig. 6. Relaxation Rates  $\gamma_F^{85}$  as a Function of Normalized Probe Light Intensity. The solid lines are least-squares fits to the data for the cases of probing the population in either the  $F = 2$  or  $F = 3$  hyperfine level.

Table 1. Experimental Results for One Dichlorodimethylsilane Coated Resonance Cell

Isotope	Probing F = a		Probing F = b	
	$k_a^A$ (sec <sup>-1</sup> )	$\gamma_o^A$ (sec <sup>-1</sup> )	$k_b^A$ (sec <sup>-1</sup> )	$\gamma_o^A$ (sec <sup>-1</sup> )
Rb <sup>85</sup>	671 ± 21	854 ± 11	945 ± 57	840 ± 29
Rb <sup>87</sup>	475 ± 70	698 ± 36	904 ± 71	716 ± 36

$\text{sec}^{-1}$  and  $\gamma_s^{87} = 620 \text{ sec}^{-1}$ . These values then yield  $\rho = 1.23 \pm 0.06$ , where the uncertainty quoted with this value is computed from the experimental uncertainties associated with the  $\gamma_o^A$  values only, and is presented simply to show that  $\rho$  is statistically different from unity.

With regard to the effect of the uncertainties associated with  $\gamma_{\text{ex}}$  and  $\gamma_{\text{st}}$  on  $\rho$ , it should be noted that even in the worst case (where one assumes that spin exchange and stem relaxation are negligible) one obtains  $\rho = 1.20 \pm 0.05$  which is still statistically different from unity. In actuality our estimates of  $\gamma_{\text{ex}}$  and  $\gamma_{\text{st}}$  are probably too large, since the alkali density is most likely less than  $1.8 \times 10^{10} \text{ cm}^{-3}$ , and since not every collision with the stem region results in an impact with the condensed ring of rubidium. Thus, the actual mean experimental value of  $\rho$  is probably somewhere between 1.20 and 1.23.

In order to more fully substantiate the claim that the above value of  $\rho$  was indicative of the rubidium-DMS surface interaction, the following experiments were performed:

1. Several cells were studied, and in each cell  $\rho$  had nearly the same value.
2. A spherical cell was studied whose radius was approximately three times greater than the normal radius of  $\sim 1.3 \text{ cm}$ . Both  $\gamma_o^{85}$  and  $\gamma_o^{87}$  decreased significantly, implying that the light-independent relaxation rate was a decreasing function of the time of flight across the resonance cell.<sup>9</sup>
3. An uncoated resonance cell was studied. The value of  $\gamma_o^A$  was roughly an order of magnitude greater ( $\sim 5000 \text{ sec}^{-1}$ ) than in the dichlorodimethylsilane coated cells, and  $\rho$  was found to be  $1.03 \pm 0.04$ . This implied that the coated cell value of  $\rho$  was related to the DMS surface.
4. A special cell containing a barium getter was fabricated, and  $\rho$  was measured both prior to and after flashing. Recent measurements indicate that in the presence of an alkali metal the DMS surface produces a trace gaseous product containing  $\text{Si}(\text{CH}_3)_2$  groups, and that this product can be detected by observing the width of Dicke-narrowed O-O hyperfine transition line shapes.<sup>19</sup> For measurements both prior to and after flashing  $\rho$  was found to be 1.2, even though linewidth indications showed a significant decrease in buffer gas density. Thus, any gaseous product in the resonance cells had a negligible influence on the measured value of  $\rho$ .

## V. DISCUSSION

For the relaxation of rubidium hyperfine polarization on alkane surfaces Bouchiat and Brossel found  $\rho = 1.31$ , which is in very close agreement with the present experiment's DMS  $\rho$  value of 1.23. Thus, in light of Eq. (3) it would appear that alkane surfaces and DMS surfaces have similar interaction strengths and correlation times with respect to alkali spin-polarization relaxation. To quantify this similarity, however, it is necessary to first make some statement as to the sensitivity of  $\rho$  to variations in either  $\tau_{c1}$  or  $\beta$ . To estimate this sensitivity the two parameters were varied about the values quoted by Bouchiat and Brossel,<sup>5</sup> and the effect on  $\rho$  was noted. In this way it was found that if  $\tau_{c1}$  or  $\beta$  varied by more than a factor of 2,  $\rho$  would be outside of the range  $1.15 < \rho < 1.60$ . Thus, the results from the present study would suggest that the values of  $\tau_{c1}$  and  $\beta$  for alkali spin-polarization relaxation on DMS surfaces are probably within a factor of 2 of the corresponding alkane surface values. Furthermore, taken together, the near equivalence of the  $\tau_{c1}$  and  $\beta$  values for the two surfaces implies that the ratio  $h_2^2 \tau_{c2}^2 / h_1^2$  is nearly equal for the two surfaces.

Since  $h_1$  is the rms magnetic field amplitude for the dipole-dipole interaction, it is a function of the various dimethylsiloxane nuclear spins. However, ignoring trace quantities of  $\text{Si}^{29}$  (4.7%) and  $\text{O}^{17}$  (0.04%), the nuclear spins of the naturally occurring silicon and oxygen isotopes are zero.<sup>20</sup> Thus, the rms magnetic field amplitude of the dipole-dipole interaction  $h_1$  is determined by the methyl group's protons as in the alkane case. Furthermore, since  $\tau_{c2}$  is related to surface vibrational periods, and since bond strengths and atomic weights for DMS and alkane surface molecules should not be grossly different, one does not expect much difference in the two surfaces' values of  $\tau_{c2}$ . By this line of argument we arrive at the conclusion that the similarity of  $\tau_{c1}$  and  $\beta$  for DMS and alkane surfaces implies the near equivalence of the spin-orbit rms magnetic field amplitude  $h_2$ , which could only be the case if the higher Z elements (silicon and oxygen) had a small effect on the spin-orbit interaction. This indicates that the

outermost functional group of an organic surface molecule has the primary influence on alkali spin-polarization surface relaxation, most likely as a result of steric hindrance. If the alkali atom is restricted to interact with only the surface methyl groups, then the similarity of DMS and alkane surface interaction strengths and correlation times follows directly.

If one now considers the magnitudes of the raw relaxation rates measured by Bouchiat and Brossel, which after correcting for differences in cell size were  $\sim 7 \text{ sec}^{-1}$ , it would appear that there is roughly a two-orders-of-magnitude difference between the alkane and DMS surface relaxation rates. This discrepancy is puzzling given the near equivalence of the  $\rho$  values and the above argument, but is the same type of phenomenon one encounters when one compares relaxation rate measurements from samples of the same type of surface. In order to try to understand this phenomenon, we can postulate several likely mechanisms for the difference in rates, and then see how the consequences of the mechanisms compare with the experimental results.

One explanation for the relaxation rate discrepancy is that the degree of DMS substrate coverage in the present experiment is much less than that obtained by Bouchiat and Brossel with the alkanes. Thus, in the present experiment one would conclude that the alkali atom has a non-negligible probability of impacting a surface region of bare glass, which was shown in the present experiment to be highly depolarizing. If we let  $f$  be the fractional surface area of bare glass, and assume that the DMS surface relaxation rates should be equal in magnitude to those measured by Bouchiat and Brossel for the alkane surfaces, then the  $\gamma_S^A$  obtained in the present experiment would have the form

$$\gamma_S^A = 700 \text{ sec}^{-1} = 5000 f \text{ sec}^{-1} + 7(1-f) \text{ sec}^{-1}$$

where the first term on the right is the contribution to  $\gamma_S^A$  from bare glass relaxation and the second term is the contribution from the DMS surface. In this way we would conclude that  $f = 0.14$ . However, since bare glass surface relaxation shows no isotope specificity, such a large fractional surface area of bare glass would imply that the present experiment should have yielded

a  $\rho$  value of unity. This is obviously contrary to experimental fact, so that an explanation of the relaxation rate discrepancy based on the hypothesis of incomplete substrate coverage must be rejected.

In the same vein one might attempt to explain this discrepancy by postulating some additional surface relaxation mechanism for the present experiment. As for the hypothesis of incomplete surface coverage, the observed relaxation rate would then be the sum of a rate associated with the additional mechanism and the rates of the dipole-dipole/spin-orbit combination. However, in order to be consistent with the measured value of  $\rho$ , this additional mechanism would have to exhibit the same degree of isotope specificity as the dipole-dipole/spin-orbit combination. This would be extremely fortuitous. It therefore seems likely that the cause of the discrepancy lies elsewhere.

The most reasonable explanation that is left for this discrepancy is that the adsorption time of alkali atoms on the present experiment's DMS surface is longer than that in Bouchiat and Brossel's work, specifically, roughly 100 times longer. Since the adsorption times, and hence the surface relaxation rates, are an exponential function of the adsorption energy<sup>10</sup> [i.e.,  $\gamma_s^A \sim \exp(-E_a/kT)$ , where  $E_a$  is the adsorption energy], this would imply an adsorption energy for the present experiment roughly 0.1 eV greater than that of Bouchiat and Brossel. This difference in the adsorption energy is reasonable given the range of typical physisorption energies,<sup>10</sup> and could result from either a fundamental difference in the DMS-alkali and alkane-alkali adsorption forces, or the manner in which the surfaces were prepared.<sup>13</sup> However, considering Eq. (2) in light of the similarity of  $\rho$  values obtained for alkane and DMS surface relaxation, the observation by Bouchiat and Brossel<sup>7</sup> of equivalent raw relaxation rates for alkane and DMS surfaces would imply that in at least one case it was possible to obtain equal alkali adsorption energies for DMS and alkane surfaces. Thus, we conclude that the difference in adsorption energies is related to surface preparation. Perhaps in the present study the surface preparation conditions favored a rougher DMS surface, which could be expected to increase the adsorption energy by an amount on the order of a tenth of an eV.<sup>21</sup> In any event it seems reasonable to generalize this conclusion and attribute the surface relaxation rate variations, for samples of the same type of surface, to variations in the adsorption time resulting from the surface's preparation.

## VI. SUMMARY

In the present study surface relaxation rates of rubidium hyperfine polarization 1-S were measured in Pyrex resonance cells coated with dichlorodimethylsilane. The parameter of interest, however, was the ratio of Rb isotopic wall relaxation rates  $\rho$ , since it was recognized that this was an easily measured and fairly sensitive parameter for comparing alkali relaxation mechanisms on various organic surfaces. By comparing the  $\rho$  values obtained in the present study for alkali spin-polarization relaxation on DMS surfaces with those obtained for relaxation on alkane surfaces, it was possible to qualitatively enhance the overall picture of alkali spin-polarization relaxation on organic surface coatings. Specifically, the following points were put forth:

1. The outermost functional group of an organic surface molecule has the primary influence on the mechanism of spin-polarization surface relaxation; and
2. The variation in magnitude of spin-polarization surface relaxation rates observed among different samples of the same type of surface can be most reasonably explained as arising from a variation in adsorption times, rather than as arising from a fundamental difference in the relaxation mechanism.

## REFERENCES

1. P. R. Muessig and G. J. Diebold, *Surf. Sci.* 165, L59 (1986).
2. X. Zeng, E. Miron, W. A. Van Wijngaarden, D. Schreiber and W. Happer, *Phys Lett.* 96A, 191 (1983).
3. D. R. Swenson and L. W. Anderson, *Nucl. Instrum. & Methods* B12, 157 (1985).
4. H. G. Robinson and C. E. Johnson, *Appl. Phys. Lett.* 40, 771 (1982); P. W. Zitzewitz and N. F. Ramsey, *Phys. Rev. A* 3, 51 (1971).
5. M. A. Bouchiat and J. Brossel, *Phys. Rev.* 147, 41 (1966).
6. Compare: H. M. Goldenberg, D. Kleppner and N. F. Ramsey, *Phys. Rev.* 123, 530 (1961); C. O. Alley, in *Advances in Quantum Electronics*, ed. J. R. Singer (Columbia University Press, New York, 1961), pp. 120-127; and Ref. 7. See also Ref. 2.
7. M. A. Bouchiat and J. Brossel, *Compt. Rend.* 254, 3828 (1962).
8. D. W. Sindorf and G. E. Maciel, *J. Am. Chem. Soc.* 105, 3767 (1983).
9. W. Happer, *Rev. Mod. Phys.* 44, 169 (1972).
10. J. H. deBoer, *The Dynamical Character of Adsorption*, (Clarendon Press, Oxford, 1953).
11. W. J. Herzberg, J. E. Marian and T. Vermeulen, *J. Colloid Interface Sci.* 33, 164 (1970).
12. R. A. Bernheim, *J. Chem. Phys.* 36, 135 (1962).
13. G. M. Khan, *Can. J. Chem.* 50, 125 (1972).
14. W. B. Hawkins, *Phys. Rev.* 98, 478 (1955).
15. X. Zeng, Z. Wu, T. Call, E. Miron, D. Schreiber and W. Happer, *Phys. Rev. A* 31, 260 (1985).
16. T. J. Killian, *Phys. Rev.* 27, 578 (1926).
17. J. C. Camparo and K. P. Frueholz, *Phys. Rev. A* 31, 1440 (1985).
18. N. W. Ressler, R. H. Sands and T. E. Stark, *Phys. Rev.* 184, 102 (1969).
19. J. C. Camparo, R. P. Frueholz and B. Jaduszliwer, to be published.

20. D. T. Goldman, in American Institute of Physics Handbook, edited by D. E. Gray (McGraw-Hill, New York, 1972), ch. 8b.
21. J. H. de Boer, in Advances in Colloid Science Volume III, edited by H. Mark and E. J. W. Verwey (Interscience Publishers, Inc., New York, 1950), Sec. III.

## LABORATORY OPERATIONS

The Aerospace Corporation functions as an "architect-engineer" for national security projects, specializing in advanced military space systems. Providing research support, the corporation's Laboratory Operations conducts experimental and theoretical investigations that focus on the application of scientific and technical advances to such systems. Vital to the success of these investigations is the technical staff's wide-ranging expertise and its ability to stay current with new developments. This expertise is enhanced by a research program aimed at dealing with the many problems associated with rapidly evolving space systems. Contributing their capabilities to the research effort are these individual laboratories:

Aerophysics Laboratory: Launch vehicle and reentry fluid mechanics, heat transfer and flight dynamics; chemical and electric propulsion, propellant chemistry, chemical dynamics, environmental chemistry, trace detection; spacecraft structural mechanics, contamination, thermal and structural control; high temperature thermomechanics, gas kinetics and radiation; cw and pulsed chemical and excimer laser development including chemical kinetics, spectroscopy, optical resonators, beam control, atmospheric propagation, laser effects and countermeasures.

Chemistry and Physics Laboratory: Atmospheric chemical reactions, atmospheric optics, light scattering, state-specific chemical reactions and radiative signatures of missile plumes, sensor out-of-field-of-view rejection, applied laser spectroscopy, laser chemistry, laser optoelectronics, solar cell physics, battery electrochemistry, space vacuum and radiation effects on materials, lubrication and surface phenomena, thermionic emission, photo-sensitive materials and detectors, atomic frequency standards, and environmental chemistry.

Computer Science Laboratory: Program verification, program translation, performance-sensitive system design, distributed architectures for spaceborne computers, fault-tolerant computer systems, artificial intelligence, microelectronics applications, communication protocols, and computer security.

Electronics Research Laboratory: Microelectronics, solid-state device physics, compound semiconductors, radiation hardening; electro-optics, quantum electronics, solid-state lasers, optical propagation and communications; microwave semiconductor devices, microwave/millimeter wave measurements, diagnostics and radiometry, microwave/millimeter wave thermionic devices; atomic time and frequency standards; antennas, rf systems, electromagnetic propagation phenomena, space communication systems.

Materials Sciences Laboratory: Development of new materials: metals, alloys, ceramics, polymers and their composites, and new forms of carbon; non-destructive evaluation, component failure analysis and reliability; fracture mechanics and stress corrosion; analysis and evaluation of materials at cryogenic and elevated temperatures as well as in space and enemy-induced environments.

Space Sciences Laboratory: Magnetospheric, auroral and cosmic ray physics, wave-particle interactions, magnetospheric plasma waves; atmospheric and ionospheric physics, density and composition of the upper atmosphere, remote sensing using atmospheric radiation; solar physics, infrared astronomy, infrared signature analysis; effects of solar activity, magnetic storms and nuclear explosions on the earth's atmosphere, ionosphere and magnetosphere; effects of electromagnetic and particulate radiations on space systems; space instrumentation.

END

DATE

FILMED

DTIC

6-88